Journal of Newviews in Engineering and Technology (JNET)
Vol 2, Issue 1, March, 2020
Available online at http://www.rsujnet.org/index.php/publications/2020-edition

Standard Techniques of Stress Corrosion Cracking Testing: A Review

T. N. Guma*, E. O. Ajayi, and M. H. Mohammed
Department of Mechanical Engineering Nigerian Defense Academy, Kaduna, Nigeria
*Email: tnguma@nda.edu.ng

ABSTRACT:

This paper aims to provide a compendium of basic information that is easy to read and grasp and readily available for consultation by: students, engineers, and researchers who are not yet much experienced in stress corrosion cracking (SCC) testing but need such information for furthering their knowledge on the subject. SCC has been reaffirmed as an unpredictable dangerous form of corrosion that is often inevitable in engineering service of equipment, vessels, vehicles, buildings, etc.; even with their high technological designs. Proper SCC testing is noted to be crucial for providing threshold tensile stress information for reliable environmental SCC prevention of critical engineering structural components in service. Various standard techniques of SCC testing from the literatures have been reviewed, elucidated with few recent previous researches by some practitioners, and presented. The review has shown that basically, SCC testing involves procurement of test materials in wrought form, and production of specimens to consistent dimensions and uniform smooth surface finish. Other noted essential issues involved in SCC testing are removal of residual stresses in specimens before testing them, and chemical composition and morphological characterization of specimens before and after exposing them in the test environment for determined durations. The paper shows that about 90% of SCC tests are done under constant elastic tensile strain or load with smooth bent beam, U-bend, C-rings, and pre-cracked tensile specimens against strain rate techniques. In order to obtain better applicable test results, it is advisable to always conduct tests with a given material type under different elastic stresses in each given environment using two or more different standard specimen preparation, characterization, and straining techniques to get optimal tensile stresses or strains by overall analysis of results.

Keyword: Calamity prevention, Corrosive environments, Proper test information, Structural components protection, Tensile SCC threshold stresses.

Cite This Article: Guma, T. N., Ajayi, E. O., and Mohammed, M. H. (2020). Standard Techniques of Stress Corrosion Cracking Testing: A Review. *Journal of Newviews in Engineering and Technology (JNET)*, 2 (1), 58-72.

1. INTRODUCTION:

Corrosion is a serious unavoidable natural degradation mechanism which impairs serviceability of engineering materials (Guma *et al.*, 2017). Corrosion directly or indirectly menace every facet of our economy and engineering technology with an estimated total yearly global cost of 2.5 trillion Dollars, equivalent to about 3.4% of the world's gross domestic product (Eng. 360, 2016; Guma *et al.*, 2017; NACE Int., 2016). The greater part of this cost stems from corrosion prevention or alleviation practices and researches (Guma *et al.*, 2017). Implementing corrosion prevention or control best practices can result in global savings of 15 to 35% of the total yearly global cost of corrosion (NACE Int., 2016). Corrosion testing is an important part of the total corrosion prevention or control program. It provides useful information for selection of better materials, and protection of low corrosion-resistant ones for optimal services in various types of environments. Corrosion testing is however a complex technology-involving exercise that requires techniques, expertise, and patience to accomplish with practicable results (Tait, 2012).

Different forms and types of corrosion are encountered in engineering use of materials but one highly detestable type that requires some distinct approaches for test-evaluating is SCC. SCC is a form of corrosion that is due to conjoint synergistic interaction of static tensile stress below the yield point of a material but above a critical value and corrosive environment which leads to formation and increment in sizes of cracks that would not have developed by the action of stress or environment alone (Guma *et*

al., 2014; NPL, 2020). The cracks can be inter-granular by proceeding along the grain boundaries of materials or trans-granular without noticeable preference for boundaries. SCC starts from corrosion sites on material surfaces and progresses into a brittle manner. Adjusting either the material type or tensile stress level or the environment type can change SCC status to no SCC or vice versa (Guma *et al.*, 2014). SCC is more known to be associated with metallic alloys, polymers, ceramics, glass, and concretes other than pure materials but the main concern is for structural materials especially metal components that are designed to be subjected to appreciable tensile stress levels in service. The environment under which SCC occurs is either the permanent service environment such as sea water, surf beaches, acidic soils, and corrosive atmospheres. Other environments are industrial or domestic liquids, synthetic and natural chemicals, human and animal bodies and fluids or waste products from them, and operations such as system cleaning which can leave corrosive residue on materials (Guma & Ajayi, 2019).

In emerging technologies, engineers have been making every effort to efficiently use less costly materials and increase working stresses but SCC has been a serious stumbling block to structural reliability even in the face of proper designs involving some material types. SCC can produce a marked loss of mechanical strength with little material loss. The damage done by it is not obvious to casual inspection and it can trigger mechanical fast fracture and catastrophic failure of components and structures after a period of satisfactory service (Guma *et al.*, 2014; NPL, 2020).The stresses that cause SCC are either produced as a result of the operating conditions in service use of material components and/or residual stresses introduced in the components during their manufacturing. Stresses that cause SCC can be very much lower than the material yield strength but most conventional engineering designs are based on yield strengths without or with some factors of safety which unknowingly may not address some stresses that cause SCC.

The devastating consequences of SCC have given rise to interminable researches in industries and academia involving testing SCC susceptibilities of critical engineering materials in various corrosive environments under various stress conditions to establish needful threshold stresses for preventing or mitigating SCC of such material components in such environments by correct design and/or use of other protective methods, and selection of better alternative materials (ASM, 1998; Chatterjee, 1995; Gerhardus, 2019; Ramamurthy & Atrens, 2013). SCC testing is critical for structural materials of many engineering systems such as; aircrafts, road vehicles, storage tanks, pipelines, commonly used vessels in chemical processing plants and petrochemical refineries, and power plants (Guma *et al.*, 2014; NPL, 2020). The outstanding difference between SCC testing and other types of corrosion testing is that, in SCC testing; specimens are subjected to requisite tensile stresses or straining or loadings while under immersion in the test environment for few days to years depending on whether it accelerated or service or field tests.

This paper presents a literature review of standard techniques used for SCC testing as it concerns specimen in terms of:

i. Material requirements.
ii. Surface finish and size
iii. Chemical composition and morphological characterization.
iv. Removal of residual stresses.
v. Tensioning or straining while under immersion in the test media.

The aim of this paper is to provide a compendium of basic information that is readily available for consultation by students, engineers, and researchers who are not yet much experienced in SCC testing and need the information for furthering their knowledge on the subject.

2. GROUNDWORK TO SCC TESTING

SCC specimens can be divided into two categories; smooth, and pre-cracked or notched type. Further distinctions can be made in the loading mode such as constant extension or strain rate, tests on statically loaded smooth specimens, slow strain-rate testing (SSRT), and tests on statically loaded pre-cracked specimens. It has been estimated that 90% of all SCC tests is accomplished with either constant extension or strain, or constant deflection, or pre-cracked specimens while under immersion in the test environments or media against the strain rate technique (Ramamurthy & Atrens, 2013).

During production process, wrought alloys are predominantly elongated with their grains in the longitudinal direction. As a result, SCC of wrought alloys is generally known to be more facilitating by their grain alignments than their castings (Gerhardus, 2019; Ramamurthy & Atrens, 2013). It is therefore important to be using wrought products for SCC testing and know how to relate direction of applied stress to the grain-alignment direction of alloys. It is also generally known that the resistance to SCC is less when stress is applied to wrought metal specimens in the transverse direction. For easier crack nucleation and propagation, the applied stresses need to be in the short transverse or thickness direction of prepared specimens (Chatterjee, 1995; Ramamurthy & Atrens, 2013).

Other parameters that play important role in SCC testing are chemical compositions and surface conditions of specimens, and presence of residual stresses. For consistency of specimens and correct comparative analysis of test results; it is important to chemically and morphologically characterize specimens before and after SCC tests using suitable techniques such as; scanning electron microscopy (SEM), energy-dispersive spectroscopy (EDS), Auger electron spectroscopy, Fourier transform infrared spectroscopy (FITR), Raman spectroscopy, wavelength-dispersive spectroscopy (WDS), atomic emission spectroscopy, x-ray photoelectron spectroscopy (XPS), time-of-flight secondary ion mass spectrometry, and chromatography (Ingo *et al.*, 2018). For correct test information it is also required that residual stresses in produced specimens should be removed or relieved. Residual stresses can be measured by x-ray diffraction (XRD) analysis and removed or relieved using thermal methods such as stress relief annealing, normalizing, and tempering; and mechanical methods such as shot peening, and laser peening (ASM, 1998; Prabhuraj *et al.*, 2017).

The formation and propagation of stress-corrosion cracks greatly depends on initial surface responses of components or specimens because all cracks turn to originate at rough sites or propagate from initial cracks. Uniform smoothness of specimens is therefore necessary for comparability of test results among specimens in SCC testing. Desired smoothness levels can be achieved by machining and use of various means and ratings of abrading and chemical treatments of surfaces. In preparing smooth surfaces for SCC testing, it is very important that all machining marks and scratches should be removed perpendicular to the loading direction in conformity with the grain-alignment direction of wrought alloys (Gerhardus, 2019; Ramamurthy & Atrens, 2013).

3. COMMON CONSTANT-STRESS OR STRAIN SCC TESTING TECHNIQUES:

The common constant-stress or strain SCC-testing techniques are based on bent-beam, U-bend, C-ring, and tensile specimens. The selection of the specific specimen types depends on their ease of production to accurate form, available environmental exposure space, affordability, and the planned test time (ASTM G-38 2013; ASTM G-30 & G39-99, 2016; Gerhardus, 2019).

3.1 Bent-Beam Specimens:

Bent-beam specimens are designed for SCC testing at stress levels below the elastic limits of metallic alloys (ASTM G39-99, 2016). The

Journal of Newviews in Engineering and Technology (JNET)
Vol 2, Issue 1, March, 2020
Available online at http://www.rsujnet.org/index.php/publications/2020-edition

different types of bent-beam specimens are the double-point, three-point, four-point and double beam loaded specimens. For all bent beam specimens, the specimen materials have to be in the form of flat-extruded sheet or plate, and wires. The use of bent-beam specimen with plate materials is however difficult because more rigid fixtures must be built to accommodate the specimens. The specimen holders of bent beam specimens are required to be rigid and made of the same metal as the specimen to avoid any galvanic corrosion. If the holder is made of a different metal from the specimen, it is desirable that it should be electrically insulated at its points of contact with the specimen or the entire holder should be made of a nonmetallic material (ASTM G39-99, 2016). The ASTM G39-99, 2016; covers standard practice for preparation and use of all bent-beam stress-corrosion test specimens.

3.1.1 Two-point loaded bent beam:

Two-point loaded bent beam specimen is useful for SCC testing of thin sheet or wire materials that do not deform plastically when bent such that $(L-H)/H$ is between 0.01 and 0.50 (ASTM G39-99, 2016). Where; L = length of specimen, and H = distance between the specimen supports; all in millimeters (mm) as shown in Fig. 1 for the two point-loaded bent beam specimen.

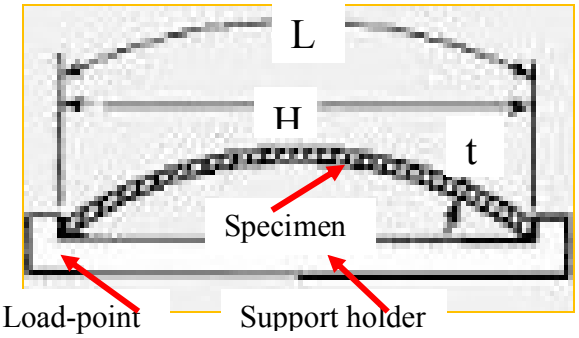

Fig.1: Two-point loaded bent specimen (ASTM G39-99, 2016; Gerhardus, 2019)

The maximum stress (σ) in mega-Pascals (MPa) in the specimen which occurs at the midpoint of the specimen between it supports and decreases to zero at the specimen ends at the supports is given by equation 1 (ASTM G39-99, 2016).

$$\sigma = 4E(2E-K)\left[\frac{k}{2} - \frac{2E-K}{12}\left(\frac{t}{H}\right)\right]\frac{t}{H} \qquad (1)$$

Where: t = thickness of specimen in millimeters (mm), E is the Young's modulus of the specimen material in Newtons per square millimeter (N/mm^2), and

$$\frac{L-H}{H} = \left(\frac{K}{2E-K}\right) - 1 \qquad (2)$$

Equation (2) can then be used to determine the value of K the chosen value of $\frac{L-H}{H}$.

$$k = \sin(\theta/2) \qquad (3)$$

θ = maximum slope of the specimen, that is, at the end of the specimen.

Specimen thickness of about 0.8-1.8 mm and holder span of 177.8-215.9 mm have been found very suitable when working with very high strength steels and aluminum alloys with applied stresses ranging from about 205MPa for aluminum to 1380MPa for steel (ASTM G39-99, 2016).

3.1.2 Three-point loaded bent beam:

Three-point loaded bent specimen types are commonly used for SCC testing because they facilitate easy application of load with ability to load the same support holder for different required specimen stresses. The three-point loaded bent beam specimen is shown in Fig. 2.

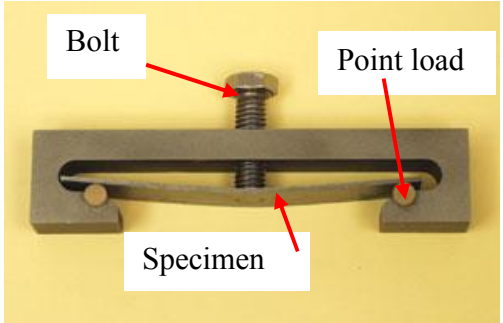

Fig.2: Three-point loaded bent specimen assembly (ASTM G39-99, 2016; Gerhardus, 2019)

Journal of Newviews in Engineering and Technology (JNET)
Vol 2, Issue 1, March, 2020
Available online at http://www.rsujnet.org/index.php/publications/2020-edition

The specimen is required to be a flat strip typically 25-51- mm width and 127-254- mm length. Choice of the specimen thickness depends on the mechanical properties and available product form of the material. In usage, the specimen is supported at its ends and bent by forcing a screw equipped with a ball or knife-edge tip against the specimen at its mid-point between the end supports as shown in Fig.2. Stresses in the bent specimen vary from 0 at the supports to maximum at its mid-span. The maximum elastic stress at mid-span in the outer fibers of the specimen is given by equation 4 (ASTM G39-99, 2016; Gerhardus, 2019).

$$\sigma = \frac{\epsilon E t y}{H^2} \quad (4)$$

Where; σ = maximum tensile stress in MPa, E = modulus of elasticity of the specimen material in N/mm^2, t = thickness of specimen in mm., y = maximum deflection of the specimen in mm, and H = distance between outer supports in mm. Equation 5 is based only on small deflection for which y/H is less than 0.1. In sheet gage bent-beam specimens where deflections are usually large, equation 4 is approximate. To obtain more accurate stress values with sheet gage specimens, a similarly made and stressed prototype specimen, equipped with strain gages can be used for calibration (ASTM G39-99, 2016).

3.1.3 Four-point loaded bent specimens:

The advantage of the four-point bent specimen is that it provides consistent tensile stress over appreciably large area of the specimen. The specimen is supported at its both ends and bent by forcing two inner located supports against it as shown in Fig. 4. The four-point bent specimen facilitates maintenance of tensile stresses during crack growth in tests. Stress is applied to the four-point bent specimen by turning the bolt as shown in Fig. 3 (Pereira *et al.*, 2019).

In the four-point loaded specimens, the maximum stress occurs between the contact points with the inner supports. In that area the stress is fairly constant. From the inner supports the stress (MPa) decreases linearly toward zero at the outer supports (ASTM G39-99, 2016). The elastic stress in the outer layer of the specimen between the two inner supports can be determined by equation 5 (ASTM G39-99, 2016; Gerhardus, 2019).

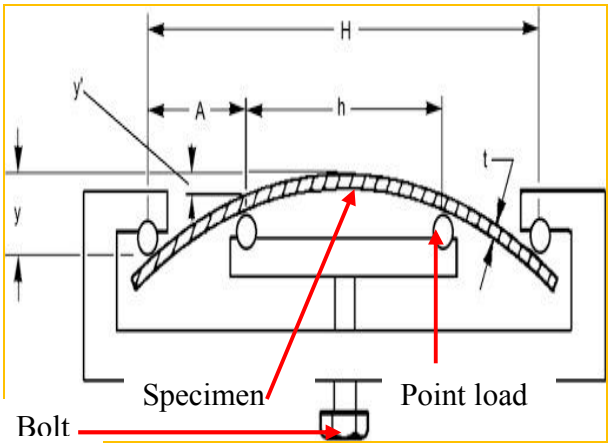

Fig. 3: Four-point loaded bent specimen (Pereira *et al.*, 2019)

$$\sigma = \frac{12Ety}{(3H^2 - 4A^2)} \quad (5)$$

Where; σ is the highest attainable tensile stress in the specimen in MPa, E is Young's modulus of the specimen material in N/mm^2, t is the specimen thickness in mm, y is the greatest specimen deflection in mm, H is the distance between the specimen's outer supports in mm, and A is the distance between the specimen's outer and inner supports in mm. The specimen is required to be a flat strip of 25-51mm width and 127-254mm length but this specification can be adjusted to meet particular needs. Such adjustment must however be made with preservation of approximate dimensional proportions. The thickness of the specimen is usually dictated by the mechanical properties of

Journal of Newviews in Engineering and Technology (JNET)
Vol 2, Issue 1, March, 2020
Available online at http://www.rsujnet.org/index.php/publications/2020-edition

the material and the product form available. Equation 5 is only based on small deflections for which y/H is less than 0.1. In sheet-gage bent-beam specimens, the deflections are usually large; so, equation 5 is approximate. To obtain more accurate stress values in such cases, a similarly made and stressed prototype specimen equipped with strain gages for calibration can be used (ASTM G39-99, 2016; Gerhardus, 2019).

3.1.4 Double-Beam Specimens (DBB):

The DBB consists of two flat strips 25-51mm width and 127-254mm length. Prepared strips are similarly bent until both ends of the strips touch using a centrally located spacer and then joined by welding or bolting the ends together to form the DBB as shown in Fig. 4. Different stress values can be induced in the same DBB by varying the spacer dimensions (ASTM G39-99, 2016; Gerhardus, 2019)

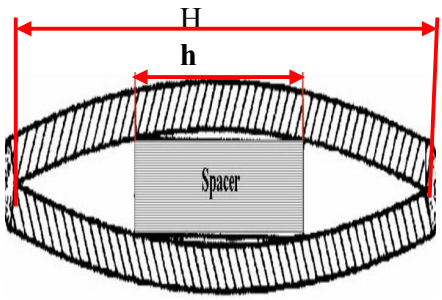

Fig.4: Welded DBB (ASM, 1998; Gerhardus, 2019)

The spacer needs to be made of the same material as the DBB or of electrically non-conducting material such as glass and ceramic to prevent any galvanic corrosion between the DBB and spacer (ASM, 1998; ASTM G39-99, 2016). The maximum elastic stress (σ) in MPa in the DBB which occurs at its mid-portion between its contact points with the spacer in its outer fibers is given by equation 6a (ASTM G39-99, 2016).

$$\sigma = \frac{3Ets}{H^2\left[\left(1-\frac{h}{H}\right)\left(1+\frac{2h}{H}\right)\right]} \quad (6a)$$

Where: E = Young's modulus of the DBB material in N/mm^2, t = thickness of the DBB in mm, s = thickness of the spacer in mm, H = across length between the middle of the DBB joints in mm, and h = the spacer length in mm. When h is chosen so that $H = 2h$, equation 6a is simplified to equation 6b (ASTM G39-99, 2016).

$$\sigma = \frac{3Ets}{H^2} \quad (6b)$$

Equations 6a&b are based on small deflections of the DBB such that, $\frac{S}{H}$ is less than 0.2. In sheet-gage bent-beam specimens, the deflections are usually large so equations 6a&b are approximate. To obtain more accurate stress values, a similarly made and stressed prototype specimen equipped with strain gages can be used for calibration (ASM, 1998; ASTM, G39-99, 2016).

3.2 U-Bend Specimens:

The U-bend specimen can be made from any metal component that is sufficiently ductile to be formed to the shape without cracking (ASTM G-30, 2016). In the constant strain method, the specimen is either stretched or bent to a fixed position at the start of SCC test. The U-bend hair pin or horseshoe types are commonly used specimen shapes for constant strain testing. U-bend specimens are prepared by bending a strip 180^o around a mandrel with a pre-determined radius. U-bend specimens can be employed for SCC testing in accordance to ASTM G-30, 2016; standard practices. Fig. 5 shows a view of U-bent specimen under stress.

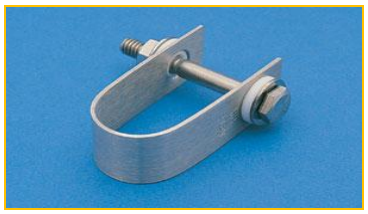

Fig 5: A view of U-bent specimen to a stress level (ASTM G-30, 2016; Metal Sample, 2020)

Journal of Newviews in Engineering and Technology (JNET)
Vol 2, Issue 1, March, 2020
Available online at http://www.rsujnet.org/index.php/publications/2020-edition

U-bend specimens have found wide use in evaluating qualitatively the SCC resistance of various alloys in various corrosive media. In the U-bend specimen test, a bolt is placed through the holes in the legs of the specimen and the specimen loaded by tightening the nut on the bolt as can be seen from Fig. 5. A good approximation of the maximum stress (σ) in MPa at the apex of the U-bend is given by equation 7 (ASM, 1998; ASTM G-30, 2016; Gerhardus, 2019).

$$\sigma = \frac{tE}{2R} \quad (7)$$

Where; $t < R$, and t is the specimen thickness in mm, R is the radius of the bend in mm, and E is the Young's modulus of the specimen material in N/mm^2. The U-bend specimen is advantageous in terms of simplicity, economy to make, and usefulness for detecting large differences between SCC resistance of different metals in the same environment or a metal in several environments (ASTM G-30, 2016; Gerhardus, 2019).

3.3 C-Ring Specimens:

C-ring specimens are versatile, and economical for quantitatively determining SCC susceptibility of alloys in different product forms. This test is particularly useful for tubing, rod, and bar in the short-transverse direction. The specimens are typically produced, prepared, and bolt-loaded to a constant strain or constant load as per ASTM G-38 standard practices. If the stresses in the outer layers of the apex of the C-ring shown in Fig.6 are in the elastic region, the stresses can be accurately calculated from equations $8a\&b$ (ASM, 1998; ASTM G-38, 2013; Gerhardus, 2019; Loto, 2017).

$$D_f = D - \Delta \quad (8a)$$

$$\sigma = \frac{4EtZ\Delta}{\pi d^2} \quad (8b)$$

Where; D is the outer diameter of the C-ring before stressing in mm, D_f is the outer diameter of the stressed C-ring in mm, σ is the attendant elastic stress in MPa, Δ is the change in D at the required stress in mm, $d = (D - t)$, t is the wall thickness of the C-ring in mm, E is the Young's modulus of the ring material in N/mm^2, and Z is the correction factor for the curved ring that depends on D/t values as shown in Fig. 7. Sizes for C-rings may be varied over a wide range, but C-rings with outside diameters (D) less than about 16mm are not recommended because of increased difficulties in machining and decreased precision in stressing (ASTM G-38, 2013).

The stress on C-ring specimens can be more accurately determined by attaching circumference and transverse strain gages to the stressed surface to obtain two strain measurements; (ε_c), and (ε_t).

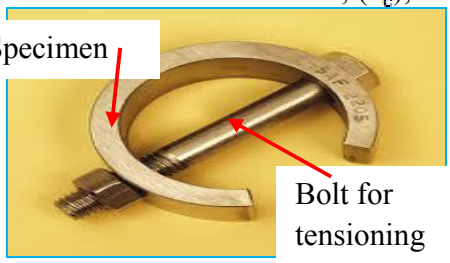

Fig. 6: C-ring specimen under stress (Metal Samples Company, 2020)

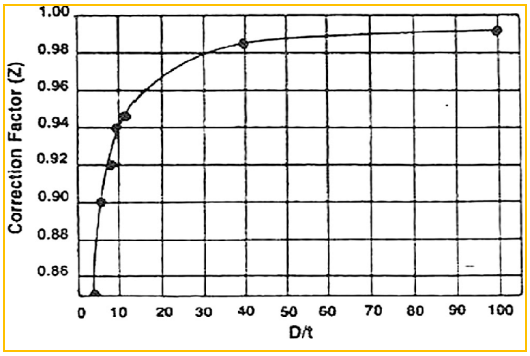

Fig. 7: Correction factors for various D/t ratios of C-rings (Loto, 2017)

The circumferential elastic stresses (σ_c) and transverse elastic stresses (σ_t) in the specimen can then be calculated by equations 9a and 9b using the strain gauge measurements (ASTM G-38, 2013; Gerhardus, 2019).

$$\sigma_c = E(1-\mu^2)(\varepsilon_c + \mu\varepsilon_t) \quad (9a)$$

$$\sigma_t = E(1-\mu^2)(\varepsilon_t + \mu\varepsilon_c) \quad (9b)$$

Where E is the Young's modulus in N/mm^2, and μ is Poisson's ratio of the C-ring material.

Journal of Newviews in Engineering and Technology (JNET)
Vol 2, Issue 1, March, 2020
Available online at http://www.rsujnet.org/index.php/publications/2020-edition

3.4 Tensile Specimens:

Use of tensile specimens is one of the most versatile methods of SCC testing, because of the flexibility permitted in; the type and size of the specimens, stressing procedures, and the range of obtainable stress levels (ASM, 1998; ASTM E-8, 2000; Gerhardus, 2019). Although both larger and smaller cross-section tensile specimens are available for SCC tests, the smaller cross-section specimens are frequently selected. However, specimens of less than about 10mm in gage length and 3 mm in diameter are not recommended except when testing wire specimens because of difficulty in producing them to accurate surface finishes and dimensions with minimal residual stresses using ordinary workshop facilities (ASM, 1998; ASTM E-8, 2000; Gerhardus, 2019).

When axially loaded in one direction in tension, the stress pattern in tensile specimens is simple and uniform and the magnitude of the applied stress can be accurately measured. Specimens can be quantitatively stressed by equipment that applies either constant strain increasing strain (ASM, 1998; ASTM E-8, 2000; Gerhardus, 2019). Tension specimens can however be subjected to a wide range of stress levels associated with either elastic or plastic strain. Because the stress system is intended to be essentially in one direction, except in the case of notched specimens; great care needs to be exercised in construction of the stressing frames to prevent or minimize bending or stresses due to torsion in the specimens (ASM, 1998; Gerhardus, 2019). The ASTM G-49 standard covers procedures for preparation and use of direct tension stress corrosion test specimens. The procedures can be used for investigating SCC susceptibility of materials in various media.

4. STATICALLY LOADED SMOOTH SPECIMENS TO FAILURE:

SCC tests are usually conducted with tensile specimens stressed to failure at various fixed stress levels in the test corrosive media with measurements of the respective times to failure (Chatterjee, 1995). The specimen can be directly loaded by hanging a suitable dead-weight load at one of its ends or by cantilevering the specimen to induce the desired constant tensile stress. Also, most of the other constant deformation specimens discussed in this paper such as two-point, three-point, and four-point loaded beam specimens can be adapted to constant load by adding a spring in them (ASTM G-49, 2000; Chatterjee, 1995). Threshold stress below which the time of failure (t_f) approaches infinity is encountered in some systems, whereas in other systems it is not observed. Time to failure (t_f) is made up of the time for crack initiation (t_i) and the time for crack propagation (t_p) as given by equation 10 (Chatterjee, 1995; Umamaheshwer Rao *et al.*, 2016).

$$t_f = t_i + t_p \quad (10)$$

By plotting various values of t_f for different applied stresses (σ) to an alloy under the same test condition in a test corrosive environment, the threshold stresses (σ_{th}) on the plot for the alloy can be established where t_f approach infinity (Chatterjee, 1995). This is for example, illustrated with test data by Prabhuraj *et al.* (2017) as shown in Fig.8.

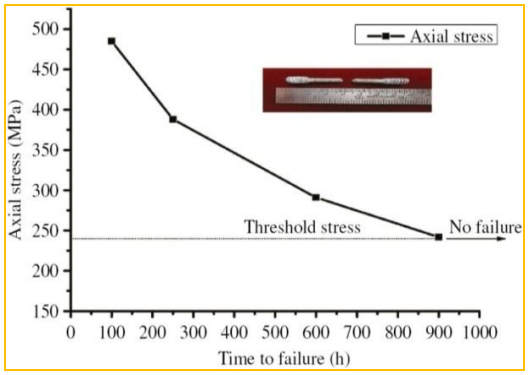

Fig. 8: Time-to-failure and applied stress relationship obtained in a constant-load type SCC test (Prabhuraj *et al.*, 2017)

In smooth specimens t_i is usually much greater than t_p, whereas in practical situations a pit or a surface roughness feature can act as an already

Journal of Newviews in Engineering and Technology (JNET)
Vol 2, Issue 1, March, 2020
Available online at http://www.rsujnet.org/index.php/publications/2020-edition

initiated crack and the question of its propagation under different variables assumes more importance. That is why the use of pre-cracked or notched specimens and the application of linear elastic fracture mechanics technique in stress corrosion crack propagation have evolved as a consequence (Chatterjee, 1995).

5. STATICALLY LOADED PRE-CRACKED TENSILE SPECIMENS:

In this testing procedure, SCC tests are often conducted with a constant applied load on pre-cracked tensile specimens and the velocity of crack propagation (V_p) as a function of stress-intensity factor (k) measured. The value of k is calculated according to equation 11 (Chatterjee, 1995).

$$k = \sigma(\sqrt{\pi})C^{0.5} \quad (11)$$

Where; σ is the applied stress, and C is the crack length. From the values of V_p and k, the threshold stress-intensity level (k_{ISSC}) below which no crack propagation is observed can then be established for the test material as shown in Fig. 9 for the general three-stage crack propagation rate that is generally observed with most materials in tests (Chatterjee, 1995; Umamaheshwer Rao *et al.*, 2016).

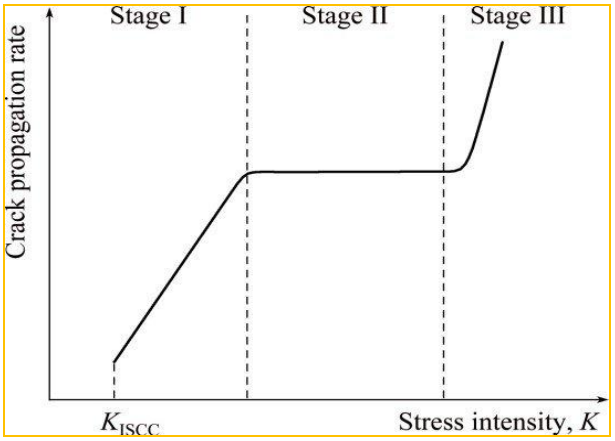

Fig.9: General relationship between stress corrosion crack velocity and stress intensity factor (Chatterjee, 1995; Umamaheshwer Rao *et al.*, 2016)

6. SLOW STRAIN RATE TESTING (SSRT):

The commonly used strain rate SCC testing technique is SSRT. SSRT is very suitable for mechanistic studies, as well as for relative ranking of SCC susceptibility of different alloys. SSRT involves use of smooth or pre-cracked tensile specimen or other suitable specimen types (Chatterjee, 1995; Ramamurthy & Atrens, 2013; Umamaheshwer Rao *et al.*, 2016). In SSRT, the specimen is exposed and strained to failure at the same temperature in both the test corrosive environment and any known SCC-inert environment for comparative assessment. In SSRT, typical specimen strain of $1x10^{-7}s^{-1}$ to $1x10^{-4}s^{-1}$ is induced with typical low motor-driven crosshead speed of 10^{-5} to 10^{-9} m/s to produce SCC and/or mechanical failure fractures of alloys. The induced specimen strain is about four orders of magnitude slower than that used in a standard tensile test (Chatterjee, 1995; Ramamurthy & Atrens, 2013; Venkatesh & Kane, 2009). From this straining, the ductility ratio which is the ratio of ductility measurement such as elongation, reduction in area, or fracture energy measured in the test corrosive environment to that obtained in the SCC-inert reference environment is determined (Chatterjee, 1995; Ramamurthy & Atrens, 2013; Umamaheshwer Rao *et al.*, 2016). The SCC susceptibility of an alloy is evaluated in terms of the time taken for failure to occur, threshold stress for cracking, the extension at failure, and/or morphology features of the fracture surface. The SSRT technique is more advantageous than the constant-strain or constant-load test methods in terms of comparatively shorter test-completion period, less cost, and simpler test procedures. Nevertheless, the SSRT technique involves more aggressive test conditions and elaborate facilities than the other SCC techniques. (Chatterjee, 1995; Ramamurthy & Atrens, 2013; Umamaheshwer Rao *et al.*, 2016; Venkatesh & Kane, 2009). SSRT tests are carried out in accordance with ASTM G-129 standard. The specimens are prepared according to ASTM G-49 and ASTM E-

8 standards (ASTM E-8, 2000; ASTM G-49, 2000; ASTM G-129, 2013).

7. REVIEWS OF EXPERIMENTAL EXAMPLES AND RESULTS OBTAINED BY OTHER RESEARCHERS:

Rahimi and Marrow (2008) noted that inter-granular stress corrosion cracking (IGSCC) causes failures in austenitic stainless steels when the appropriate electrochemical, metallurgical and mechanical conditions exist. They investigated the effects of time, applied stress, residual stress and microstructure on a population sample of short crack nuclei in sensitized type 304 austenitic stainless steel, tested under static load in an acidified potassium tetrathionate ($K_2S_4O_6$) medium. They received their material in plate form with dimension of 1m by 1m by 13mm in the mill-annealed condition with its chemical composition supplied by the manufacturer. They produced specimens of dimensions 240mm by 30mm by13mm from the plate with the length along rolling direction. They then solution annealed these blanks at 1050°C for 2 hours in air and cooled them down in air to room temperature. Subsequently, they sensitized the blanks at 650°C for 20 hours in air atmosphere and machined these sensitized solution annealed blanks parallel to the rolling plane to the final dimensions of 240×30×7mm. From there, they carried out the metallographic study of material across the thickness for both the as received and solution annealed conditions. They performed this by electro-etching the surface in 10% oxalic acid under 13-V and less than a minute conditions followed by investigation of the surfaces using an Olympus-BH2 optical microscope.

They conducted surface optimization and loading by subjecting the as-machined strips to an electro-polishing process to remove the residual stress introduced by the machining stage. The electrolyte solution they used was a mixture of acetic acid (92 % wt) and perchloric acid (8 % wt) and the cathode was stainless steel type 304 sheets with approximate dimensions of 19cm×8cm×0.5mm. They immersed the specimens in the electrolyte solution for 10, 20, 40, 60 minutes electro-polishing at 45V and optimized the electro-polishing time duration by performing XRD measurements using a Proto i-XRD portable stress diffractometer. Ultimately, they choose 60 minutes electro-polishing for all strips to attain stress free surfaces for the stress corrosion tests. In order to produce a static tensile elastic stress to perform stress corrosion cracking experiments, they choose DBBs and prepared them according to ASTM G39-99 standard. Each DBB was formed with a spacer and composed of two strips of the same microstructure and dimensions bolted at their ends. In order to obtain nominal stresses of 100MPa, 200MPa, and 260MPa in the specimens; they used spacer thicknesses of 1.5mm, 3mm, and 4mm respectively. They obtained XRD measurements on electro-polished and loaded and unloaded samples to evaluate the magnitudes of applied stresses in comparison with calculated stresses.

Koo *et al*. (2017) reported on the effect of long-term static stress on degradation of magnesium alloys and further changes in mechanical integrity of the alloys. They characterized by nominal composition and tested AZ31B (H24) and ZE41A (T5) magnesium alloys to evaluate SCC of the alloys in a physiological solution for 30 days and 90 days in accordance to the ASTM G-39 testing standard. They characterized surface morphology and micro-structure of degraded alloys using scanning electron microscopy with energy-dispersive X-ray spectroscopy and micro-computed tomography. They conducted SCC test with the two magnesium alloys in Hank's Balanced Salt solution by ASTM G-39 standard with the four-point load bent specimens. In terms of number of specimens for the SCC test, they studied 13 specimens of AZ31B out of which 3 blank specimens were used for control, 3 specimens for 30-day immersion, 3 specimens for 30-day immersion with stress, 2 specimens for 90-day immersion and 2 specimens for 90-day immersion with stress. They similarly tested the same 13 number of specimens of the ZE41A

alloy for the SCC test. They also examined 3 specimens for each alloy for tensile tests. They prepared specimens for SCC test from the magnesium alloys and mechanically polished the specimens to remove the oxide layer sequentially with 800, 1000, and 1200 grit silicon carbide paper with isopropyl alcohol. They then ultrasonically cleaned the specimens sequentially with acetone and ethanol, and dried them using nitrogen stream. They used the ASTM G-39 loading frame and 316L ASTM G-39 four-point bent beam loading clamps purchased from Metal Samples, and loaded their prepared samples on the frames to simulate tensile and compression stresses on SCC of the specimens in Hank's Balanced Salt solution.

They applied static load between the inner supports of the specimen to obtain tensile stress(σ) of 120MPa in the specimen, and calculated the required deflection to achieve the stress from the four-point load bent beam formula by ASTM G39-99, 2016 in equation 6a. They verified the accuracy of this experimental method by measuring deflection on one sample using a strain gauge. They screwed their specimens to the main loading frame and took measurement of the frame deflection with accuracy of about ±0.01mm using a dial gauge. Their results showed different mechanisms of trans-granular stress corrosion cracking (TGSCC) for the AZ31B and inter-granular stress corrosion cracking (IGSCC) for the ZE41A. They finally concluded that:

i. The ZE41A alloy was less susceptible to SCC under a long-term static load than the AZ31B alloy. Stress corrosion cracks occurred for both alloys but with different mechanisms; TGSCC for AZ31B and IGSCC for ZE41A.
ii. Static loading under long-term accelerated crack propagation which led to loss in mechanical strength of the alloys.

Pandhi *et al*. (2017) hinted that amine exchangers are widely used in gas sweetening plants for amine solution regeneration process. They conducted cracking and leakage investigation on the 304 stainless steel type plate used between absorption and stripper towers in an amine exchanger unit. They performed, micro and macro examinations on the plate, and analyzed the amine solution. They observed micro cracks on both sides of the plate, especially under the gasket region of the plate. Their results showed that the main reason of the cracking was inter-granular corrosion accompanied by stress. They concluded that high concentration of formate in amine solution, and also high level of stress under the gasket region, initiated the inter-granular corrosion and cracking.

As part of their experimental details, they performed environmental induced cracking test according to ASTM G-30 standard in lean amine solution under nitrogen blanket. In that regard; they cut, drilled, blended, and finally bolted U-bend sheet samples. They used two types of U-bend specimens for their tests of the sheet samples; one bolted for investing the effect of tension stresses on crack initiation and the other non-bolted. After one-month U-bend immersion test with the bolted and non-bolted specimens in lean amine solution as a representative of amine solutions in contact with amine exchanger plates; they found that the non-bolted specimens showed inter-granular corrosion, while inter-granular corrosion and cracking was observed for the bolted specimens. Since the bolted specimens had higher stresses than the non-bolted specimens, they confirmed the inter-granular stress assisted corrosion cracking.

Yue *et al*. (2018) assessed susceptibility of super 13Cr steel to SCC through SSRT in simulated formation water saturated with carbon dioxide (CO_2) under a high-temperature and high-pressure (HTHP) environment. By in situ electrochemical methods and surface analysis; they evaluated the evolution, morphology, and chemistry of fracture and corrosion products on the steel surface. Their results indicated that the occurrence of pitting corrosion increased SCC susceptibility of the steel. They reported that at 150°C, the degradation of a surface film induced

pitting corrosion due to an increase in anodic processes. The presence of chlorides caused film porosity, and CO_2 reduced the $Cr(OH)_3/FeCO_3$ ratio in the inner film, which further promoted chloride-induced porosity.

In the experimental process, they used a CORTEST/National Instrument VI SSRT machine to perform their SSRT on the steel surface. They used specimens of the ASTM-E8 with gauge diameters of 6.35mm and lengths of 24.4mm. Their surface preparation process of the specimen included wet grinding up to 1000 grit, ultrasonic washing using acetone followed by alcohol, and drying with ambient air temperature. They observed SCC of the super 13Cr steel at temperatures in the range of 120 °C to 150 °C in an autoclave. To fracture the specimen, it was pulled at an extension rate of 2.54×10^{-5} mm s^{-1} after the temperature reached that of the testing condition. They carried out their tests in 16-wt% NaCl under 1-MPa CO_2 atmosphere, but the control tests under constant 1-MPa in nitrogen atmosphere to provide an inert environment. They analyzed the micro-morphology of each specimen surface after fracture through scanning electron microscope (SEM) type JEOL with serial No. JSM-6510A. They compared their results of SSRT corrosion tests in terms of time to failure, maximum stress, and strain with the parameters obtained in the inert environment. They also expressed SCC susceptibility using breakage elongation, reduction of area, tensile strength, energy absorption, and fracture time of the steel at the three temperatures by comparison of the parameters. To evaluate the degree of stress corrosion; they determined the variations in strength, breaking elongation, and area reduction as well as the fracture time before and after stress corrosion.

The specimens were subjected to static loading of 90% of their actual yield strengths in conformity with the ISO 7439-2 standard, at 120°C and 150°C in a four-point bending tests with three specimens for each test in an autoclave under 1-MPa CO_2 atmosphere immersion for 30 days to determine the composition of corrosion products of the steel under stress. After each test they ultrasonically cleaned the specimens, rinsed them with de-ionized water, dried them with ambient air temperature, and stored them in desiccators. Thereto they analyzed the morphologies and elemental compositions of the corrosion products using a combination of SEM/EDS and XPS techniques.

Guma and Ajayi (2019) hinted that stress corrosion cracking (SCC) is unpredictable type of corrosion that is; often associated with calamity, and highly detested. They regretted that 300M steel is a special but notable failure-prone structural material by SCC. The aim of their study was to find out SCC mitigation extents of 300M steel by tempering and normalizing heat treatments in seven aqueous media that contained different concentrations of hydrochloric acid (HCl) and sodium chloride (NaCl) up to 17.5%. They produced 56 ASTM E-8 standard tensile test samples from procured un-heat-treated 300M steel out of which 14 were heat-treated by tempering and 14 by normalizing. They procedurally cleaned the samples to uniformly smooth surface finishes. They loaded each sample to the same maximum tensile bending stress(σ) of 1427.4MPa by cantilevering in which in the stress was determined according to equation 12 (Guma & Ajayi, 2019).

$$\sigma = \frac{32mgl}{\pi d^3} \qquad (12)$$

Where; m was mass of the hung load at the free end of the cantilevered sample, g was acceleration due to gravity = $9.81 m/s^2$, l was $52mm$ = distance of the applied load from the fixed end of the cantilevered specimen, d was the diameter of the gauge length of the cantilevered sample = $5mm$, $\sigma =$ $1427.4MPa$ was the intended stress to be applied to each sample under test. Using Equation (12), the hung mass m was evaluated to be $34.36Kg$.They immersed the loaded samples in pairs of one tempered with one un-heat-treated and one normalized with one un-

heat-treated in each of their seven prepared media under separate constant temperatures of 60°C and 100°C for one hour. Thereafter, they removed the specimens for integrity assessment with respect to internal and surface cracks by micro-examination. Their obtained results showed no SCC for all the heat-treated samples but multiple trans-granular crack features alongside craters that increased in intensity with the acid and chloride contents and propagated in the matrix structure to the surfaces for the un-heat-treated samples tested at100°C in media that contained from 14%HCl and 14% NaCl.

8. CONCLUSION:

The paper has reaffirmed that SCC is an unpredictable and highly dangerous form of corrosion that can be inevitable in engineering service of structural components even with high technological designs. Proper SCC testing is the only way of obtaining threshold stresses of critical structural components in various types of environments for: service SCC-prevention of the components by correctly designing and/or protecting the components using other corrosion-protective methods, or selecting better alternative material to the components. A literature review of standard techniques used for SCC testing has been presented as it concerns specimen in terms of:

i. Material requirements.
ii. Surface finish and size.
iii. Chemical composition and morphological characterization.
iv. Removal of residual stresses.
v. Tensioning or straining while under immersion in the test media.

The review has shown that about 90% of SCC tests are done under constant elastic tensile stress or load with smooth bent beam, U-bend, C-rings, and pre-cracked tensile specimens against strain rate techniques. The strain rate techniques, especially the SSRT technique is however seen to be more advantageous in terms of comparatively shorter test-completion period, less cost, and simpler test procedures. On the other hand, the SSRT technique is seen to require more aggressive test conditions and elaborate facilities. The review is posited for consultation by students, engineers, and researchers in academia or industries who are not yet much experienced in SCC testing and need the information for furthering their knowledge on the subject.

REFERENCES

ASM (1998). ASM Metals Handbook Corrosion testing section, Desk Edition. American Society of Metals, Materials Park, Ohio. USA.

ASTM E-8 (2000). Standard Test Methods for Tension Testing of Metallic Materials Annual Book of ASTM Standards. West Conshohocken, Pa.

ASTM G-129 (2013). Standard Test Methods for Slow Strain Rate Testing to Evaluate the Susceptibility of Metallic Materials to Environmentally Assisted Cracking. Annual Book of ASTM Standards. West Conshohocken, Pa.

ASTM G30 (2016). Standard Practice for Making and Using U-Bend Stress-Corrosion Test Specimens. ASTM Book of Standards. ASTM West Conshohocken, Pa.

ASTM G-38 (2013). Standard Practice for Making and Using C-Ring Stress-Corrosion Test Specimens. ASTM Standards. West Conshohocken, Pa.

ASTM G39-99 (2016). Standard Practice for Preparation and Use of Bent-Beam Stress-Corrosion Test Specimens, ASTM Standards, West Conshohocken, Pa, 2016.

ASTM G-49 (2000). Standard Test Methods for Preparation and Use of Direct Tension Stress-Corrosion Test Specimens. Annual Book of ASTM Standards. West Conshohocken, Pa.

Chatterjee, U.K. (1995) Stress Corrosion Cracking and Component Failure: Causes and Prevention Sadhana & Vol. 20, Part 1, 165-184.

Eng.360 (2016). Engineering360 News Desk, Albany, New York, 21 March.

Gerhardus H. Koch. (2019). Tests for Stress-Corrosion - ASM International https://www.asminternational.org/...pdf/026e7c61-4606-424e-9ade-3455865aba71.Accessed 14/06/2019

Guma, T.N. & Ajayi, E.O. (2019). Effects of Tempering and Normalizing Heat Treatments on Stress Corrosion Cracking Behaviors of Modified AISI 4340 (300M) Steel in Acidic Chloride Media. *Nigerian Research Journal of Engineering and Environmental Sciences*, 4(2), 604-616.

Guma, T.N., Atiku, S. A., and Abdullahi, & A. A. (2017). Corrosion Management and Control: Entrepreneurial Opportunities and Challenges in Nigeria. *International Journal of Engineering Research and Application,* 7(10), 14-23.

Guma, T.N., Solomon, W.C., & Sambo, H.L. (2014). Assessment of Stress Corrosion Cracking (SCC) Susceptibilities of Some Outokumpu-Produced Stainless Steels in a River Harbor Mud Using Accelerated Test. *International Journal of Engineering Sciences & Research Technology*, 3(11), 672-680.

Ingo, G.M., Riccucci, C., Pascucci, M., Messina, E., Giuliani, C., Biocca, P., Tortora, L., Fierro, G., & Di, C. G. (2018). Combined use of FE-SEM+EDS, ToF-SIMS, XPS, XRD and OM for the study of ancient gilded artefacts. *Applied Surface Science*, In press, 1-9.

Koo, Y. Jang, Y. & Yun, Y. (2017). A Study of Long-term Static Load on Degradation and Mechanical Integrity of Mg Alloys-based Biodegradable Metals. *Material Sci. Eng. B Solid State Mater Adv Techno*, 45–54.

Loto, C.A. (2017). Electrochemical Noise Evaluation and Data Statistical Analysis of Stressed Aluminum Alloy in NaCl Solution. In Press, *Alexandri Engineering Journal*.

Metal Samples Company (2020). Corrosion Monitoring Systems. www.metexcorporation.com›*aspi.* Accessed 12/04/2020.

NACE Int. (2016). NACE International, Houston, Texas, USA, 08 March.

NPL (2020). NPL Guides to Good Practice in Corrosion Control-Stress Corrosion Cracking.https://www.iims.org.uk/wp-content/uploads/2014/03/stress_corrosion cracking. Accessed 23/2/2020.

Panahi, H., Eslami, A., Golozar, M.A., Ashrafi, A., Aryanpur, M., Mazarei, M., (2017). Failure Analysis of type 304 Stainless Steel Amine Exchanger Sheets in a Gas Sweetening Plant. ELSEVIER Case Studies in Engineering Failure Analysis, Vol. 9, 87-98.

Pereira, H. B., Panossian, Z., Baptista, I.P., & Azevedo, C.R. (2019). Investigation of Stress Corrosion Cracking of Austenitic, Duplex and Super Duplex Stainless Steels under Drop Evaporation Test Using Synthetic Seawater. *Materials. Research*. 22 (2), 1-13.

Prabhuraj, P., Rajakumar, S., Lakshminarayanan, A.K., & Balasubramanian, V. (2017). Evaluating Stress Corrosion Cracking Behavior of High Strength AA7075-T651 Aluminium Alloy. *Journal of the Mechanical Behavior of Materials*, Vol. 26: Issue 3-4, 105-112

Rahimi, S., & Marrow, T.J. (2008). Influence of Microstructure and Stress on Short Inter-granular Stress Corrosion Crack Growth in Austenitic Stainless-Steel Type 304. *17th European Conference on Fracture 2008: Multilevel Approach to Fracture of Materials, Components and Structures,* 01/09/2008, 2, 1-9.

Ramamurthy, S. & Atrens, A. (2013). Stress Corrosion Cracking of High-Strength Steels. *De GRUTER Corros Rev*, 31(1), 1–31.

Tait, W.S. (2012). Corrosion Prevention and Control of Chemical Processing Equipment: In: *Handbook of Environmental Degradation of Materials*, Edited by Myer Kutz, 2nd Edition, 2012.

Umamaheshwer Rao, A.C., Vasu, V., Govindaraju, M., & Sai Srinadh, K.V. (2016). Stress Corrosion Cracking Behavior of 7xxx Aluminum Alloys: A Literature Review. *Transactions of Nonferrous Metals Society of China*, 26 (6) 1447-1471.

Venkatesh, A; & Kane, R.D. (2009). Fracture Analysis of Slow Strain Rate Test for Stress Corrosion Cracking. *NACE International, Corrosion 2009*, 22-26 March, Atlanta Georgia, 1-18.

Yue, X., Zhao, M., Zhang, L., Zhang, H., Li, D., & Lu, M. (2018) Correlation between electrochemical properties and stress corrosion cracking of super 13Cr under an HTHP CO_2 environment. *Royal Society of Chemistry Advances*, 8 (43), 24679-24689.